Satellite observations of oil spills in Bohai Sea

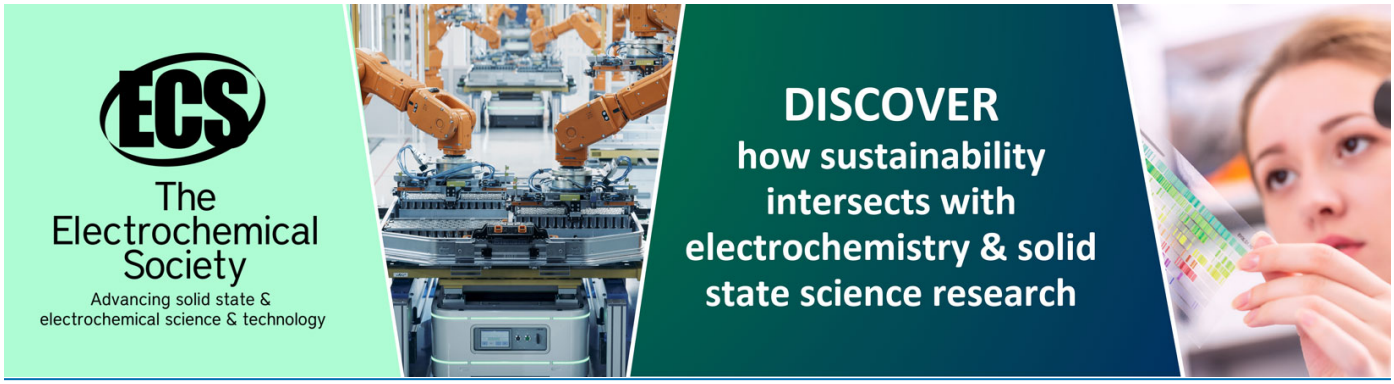

Satellite observations of oil spills in Bohai Sea

Y L Wei[1, 2], **Z Y Tang**[3], **X F Li**[2, 4]
[1] College of Marine Sciences, Shanghai Ocean University, Shanghai 201306, China
[2] International Center for Marine Studies, Shanghai Ocean University, Shanghai 201306, China
[3] East China Sea Prediction Center, State Oceanic Administration of China, Shanghai 200081, China
[4] GST at NOAA/NESDIS, College Park, MD 20740, USA

E-mail: xiaofeng.li@noaa.gov

Abstract. Several oil spills occurred at two oil platforms in Bohai Sea, China on June 4 and 17, 2011. The oil spills were subsequently imaged by different types of satellite sensors including SAR (Synthetic Aperture Radar), Chinese HJ-1-B CCD and NOAA MODIS. In order to detect the oil spills more accurately, images of the former three sensors were used in this study. Oil spills were detected using the semi-supervised Texture-Classifying Neural Network Algorithm (TCNNA) in SAR images and gradient edge detection algorithm in HJ-1-B and MODIS images. The results show that, on June 11, the area of oil slicks is 31 km^2 and they are observed in the vicinity and to the north of the oilfield in SAR image. The coverage of the oil spill expands dramatically to 244 km^2 due to the newly released oil after June 11 in SAR image of June 14. The results on June 19 show that under a cloud-free condition, CCD and MODIS images capture the oil spills clearly while TCNNA cannot separate them from the background surface, which implies that the optical images play an important role in oil detection besides SAR images.

1. Introduction

Accurate detection of oil spills is beneficial to wildlife, fisheries, resolving dispute related to liability, resource management for monitoring and conserving of marine environment. Therefore, oil spill monitoring is considered to be one of the most important applications for operational oceanography (e.g., Hackett et al. [1], Sun et al. [2], Cheng et al. [3]).

Two separate oil spill accidents occurred on June 4 and 17, 2011 at platforms B and C of Penglai 19-3 oilfield (PL19-3 hereafter), which is jointed owned by China National Offshore Oil Corporation and ConocoPhillips, located in Bohai Sea (38.37°N, 120.08°E, figure 1), China. These accidents resulted in a release of approximately 700 barrels of oil and 2,500 barrels of mineral oil-based drilling mud onto the seabed (from http://www.conocophillips.com/). Bohai Sea is a semi-closed shallow sea with average water depth of 18 m and maximum of 70 m. Due to the relatively high risk of oil spills in this region and vulnerability of the coastal zones on oil spill beaching, many studies have been carried out in this area (e.g., Sun et al. [2], Guo et al. [4], Li and Bai [5]). However, no large-scale oil spill event had occurred and been reported before June 4, 2011.

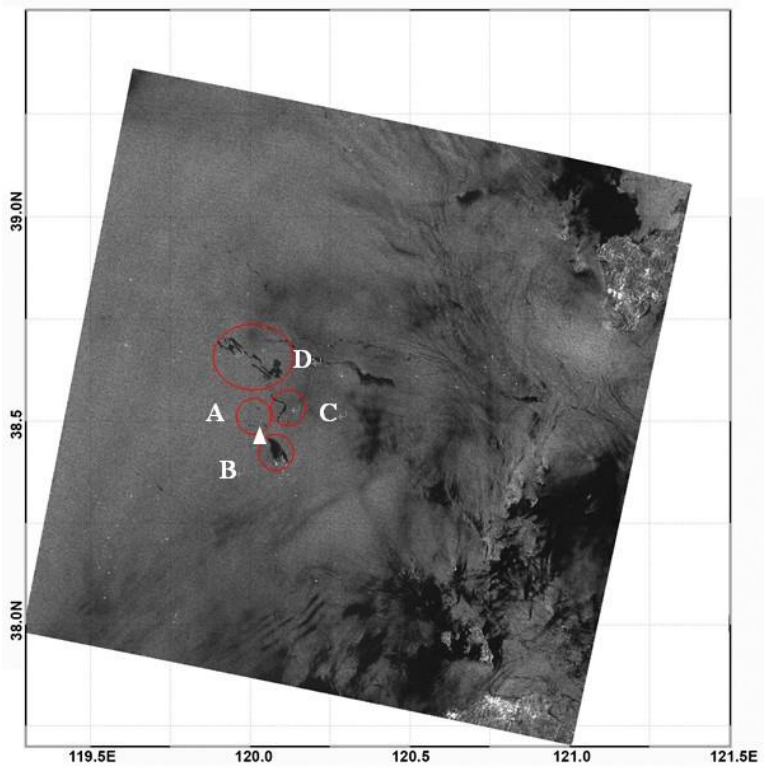

Figure 1. The remote sensing observations from ENVISAT-ASAR on June 11. The observed oil slicks on ASAR images are marked in circle with letters A-D. The triangle represents the location of PL19-3 oilfield.

With its day/night/all-weather imaging capabilities and relatively wide coverage, SAR (Synthetic Aperture Radar) has been widely used to provide valuable synoptic information about the position and size of the oil spills and seeps (e.g., Brekke and Solberg [6], Gade and Alpers [7], Ferraro et al. [8], Garcia-Pineda et al. [9], Liu et al. [10], Zhang et al. [11], Migliaccio et al. [12], Li et al. [13]). However, SAR cannot separate oil spills from other look-alikes such as upwelling, low wind and natural biogenic films and give false alarms. In addition, oil spill signature appears distinguishable in SAR images only within a certain range of wind speeds (Brekke and Solberg [6]). Hence it is desirable to complement SAR observations with multi-sensor images to identify oil spills accurately. Reviews of the capability of widely used sensors (Infrared, Ultraviolet Sensor, Microwave Radar and Sea-Viewing Wide Field-of-view Sensor) in oil spill detection are given in the literatures (Brekke and Solberg [6], Hu et al. [14], Hu et al. [15]).

The main objective of the present work is to use the PL19-3 oil spill event as an example to show that we can monitor the locations of oil slicks based on multi-sensor remote sensing images in semi-closed shallow sea. The paper is organized as follows: multiple satellite observations of oil spills are discussed in Part 2. Oil detection results are given in Part 3. Discussions and conclusions are in Part 4.

2. Satellite remote sensing observations

Remote sensing technique is the key in monitoring oil slicks on the ocean surface (Hu et al. [15], Kvenvolden and Cooper [16]). After the two PL19-3 oil spill accidents happened on June 4 and 17, 2011, images were acquired from ENVISAT Advanced SAR (ENVISAT-ASAR), NASA MODIS and a CCD camera onboard Chinese HJ-1-B satellite which was launched in September 2008.

The first available set of 3 images from ENVISAT-ASAR (wide swath mode and VV polarization) was acquired on June 11, 14 and 19, respectively. The second set of 2 images from HJ-1-B CCD camera was acquired on June 11 and 19, respectively. The 2 images from NASA MODIS as the third set were observed about 9 and 27 minutes after the HJ-1-B CCD images, respectively. The bands of 1, 2 and 3 of HJ-1-B CCD and the bands of 1, 3 and 4 of MODIS were used to generate composite

false-color images to highlight the oil slick signatures in these optical images.

Among all the sensors, MODIS provides the widest coverage (swath: 2330 km) and HJ-1-B CCD provides the highest resolution (30m). ENVISAT-ASAR provides medium coverage and also medium spatial resolution. Active microwave sensor (i.e., ENVISAT-SAR in this study) can image the ocean surface in all-weather and day/night conditions, while the optical sensors (i.e., MODIS and CCD) are affected by clouds. That implies the disadvantage of such sensors in observing oil slicks. Thus, we used the MODIS and CCD images as the auxiliary observation evidences besides SAR images.

In general, oil slicks are easy to be identified under low to moderate surface wind conditions. Oil signatures usually appear as dark patches in SAR images (see figure 1); however, they may appear as either dark or bright features in optical images depending upon a critical angle which is a function of sensor viewing geometry, Sun zenith angle and surface wind conditions (Jackson and Alpers [18]). And we can see both signatures in MODIS and CCD images we acquired. The oil signatures are all similar in shapes among optical and microwave images, which are relatively easy to separate from the background ocean surface because the wind was fairly calm at about 4-6 m/s over the entire study period, as mentioned above.

3. Oil detection results using multi-sensor images

In this study, the oil spill information from SAR images is detected using the semi-supervised Texture-Classifying Neural Network Algorithm (TCNNA, Garcia-Pineda et al. [9]). Oil spills in CCD and MODIS images are manually processed with gradient edge detection algorithm. Their locations were detected and cover areas were estimated. Figure 2 shows a combined result of the detected oil spills from the 7 satellite images acquired. We can see from the figure that the spilled oil located to the north and northwest of the PL19-3 oilfield (not shown in figure 2 for clarity, see figure 1) on June 11 has an estimated area of 31 km^2 from the SAR image (oil slicks B, C and D in figure 2).

The HJ-1-B CCD (slicks B1 and C1) and MODIS (slicks B2 and C2) images are acquired on the same day as SAR with 27 and 35 minutes delay. Compared with the SAR image, oil spills appear similar areas and patterns and move slightly northwards in about 30 minutes, which implies weak local oceanic dynamical conditions (i.e., weak surface current and wind speed). Moreover, the oil slicks in region A observed from HJ-1-B CCD and MODIS images are not detected from the SAR image using TCNNA due to the low contrast between the oil slicks and the background surface.

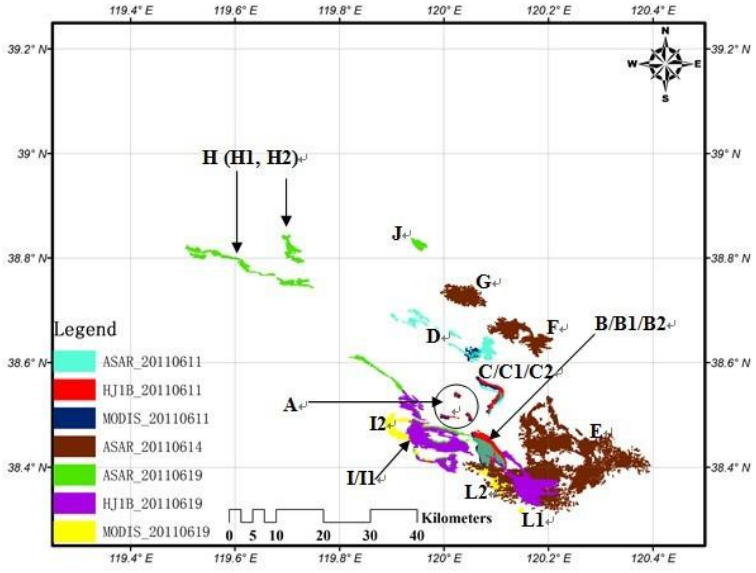

Figure 2. Extracted oil slicks based on ENVISAT-SAR, HJ-1-B CCD and MODIS images during June 11 and June 19 time period.

In SAR image acquired on June 14, oil slick appears to the east and north of the oilfield and its coverage expands dramatically to 244 km^2. We consider this (E near the oilfield) is not originated from the detected oil spills on June 11 but from newly released oil after June 11, which will be

confirmed by the model simulations in the next work.

On June 19, SAR image senses several oil slicks located in the vicinity and to the northwest of the oilfield. Note that the cloud-free parts (oil slicks L1 and L2) of HJ-1-B CCD and MODIS images acquired 33 and 170 minutes later clearly show the oil spills that are not well captured by TCNNA. The oil slick moved northwestward slightly by comparing the location of oil slick I in SAR image with I1 in HJ-1-B and I2 in MODIS images. Besides, judging from their locations, oil slicks H and J in SAR image are believed to be released from other location which will also be confirmed by model simulations in future.

4. Conclusions and discussions

In this study, oil spills from the PL19-3 oilfield accidents are detected with multiple satellite sensors (ENVISAT-ASAR, HJ-1-B CCD and MODIS). Remote sensing images captured the three-day oil slicks between June 11 and June 19, 2011. On June 11, the area of oil slicks is 31 km^2 and they are observed in the vicinity and to the north of the oilfield in SAR image. The slicks move slightly northwards in 30 minutes as shown in HJ-1-B and MODIS observations. The coverage of the oil spill expands dramatically to 244 km^2 due to the newly released oil after June 11 in SAR image of June 14. The results on June 19 show that the optical images play an important role in oil detection besides SAR images.

Another important part in oil monitoring is to predict their trajectories. In this study we only detect oil slicks from snap images. We will estimate the trajectories of the oil spills using drift model—GNOME in the next work.

Acknowledgements

SAR images were provided by ESA through Envisat projects 431 and 6133. This work was supported by Shanghai Dongfang Scholar Program. Wei was supported by Shanghai Ocean University through grants A-2400-11-0215 and B-5409-11-0005. Tang was supported by the Key Laboratory of Integrated Marine Monitoring and Applied Technologies for Harmful Algal Blooms, State Oceanic Administration, China through grant MATHAB20100303. The views, opinions, and findings contained in this work are those of the authors and should not be construed as an official NOAA or US Government position, policy, or decision.

References

[1] Hackett B, Comerma E, Daniel P, Ichikawa H 2009 *Oceanogr. Mag.* **22** 3 168-175
[2] Sun P, Gao Z, Cao L, Wang X, Zhou Q, Zhao Y and Li G 2011 *J. Ocean Univ. China* **10** 1 35-41
[3] Cheng Y C, Li X F, Xu Q, Garcia-Pineda O, Andersen O B and Pichel W G 2011 *Marine Pollution Bulletin* **62** 2 350-63
[4] Guo M 2010 *6th Int. Conf. on Natural Computation* (Icnc) 3773-77
[5] Li D and Bai L 2011 *Remote Sensing Envir. and Transp. Eng. (RSETE) 2011 Int. Conf.* 630-633
[6] Brekke C and Solberg A 2005 *Remote Sensing of Environment* **95** 1 1-13
[7] Gade M and Alpers W 1999 *Science of the Total Environment* pp. 237-238 441-448
[8] Ferraro G, Meyer-Roux S, Muellenhoff O, Pavliha M, Svetak J, Tarchi D and Topouzelis K 2009 *Int. J. Remote Sensing* **30** 3 627-645
[9] Garcia-Pineda O, Zimmer B, Howard M, Pichel W, Li X F and MacDonald I R 2009 *Canadian J. Remote Sensing* **35** 5 411-421
[10] Liu P, Li X, Qu J, Wang W, Zhao C and Pichel W 2011 *Marine Pollution Bulletin* **62** 2611-18
[11] Zhang B, Perrie W, Li X and Pichel W 2011 *Geophys. Res. Lett.* doi:10.1029/2011GL047013
[12] Migliaccio M, Nunziata F, Brown C, Holt B, Li X F, Pichel W and Shimada M 2012 *EOS* **16** 93 161-8
[13] Li X, Li C, Yang Z and Pichel W 2012 *Remote Sensing of Environment* **130** 182-187
[14] Hu C, Müller-Karger F E, Taylor C, Myhre D, Murch B, Odriozola A L and Godoy G 2003 *Eos Trans.* **84** 33 313

[15] Hu C, Li X F, Pichel W G and Muller-Karger F E 2009 *Geophys. Res. Lett.* **36** L01604
[16] Kvenvolden K A and Cooper C K 2003 *Geo. Marine Letters* **23** 140-146